Monsoon surges trigger oceanic eddy formation and propagation in the lee of the Philippine Islands

Julie Pullen,[1] James D. Doyle,[1] Paul May,[2] Cedric Chavanne,[3] Pierre Flament,[3] and Robert A. Arnone[4]

Received 26 December 2007; revised 21 February 2008; accepted 4 March 2008; published 5 April 2008.

[1] Two winter monsoon surge events (northerly and easterly) of January 2005 are captured in a one-way coupled atmosphere (8 km resolution) and ocean (3 km resolution) simulation of the Philippines region. Intensified wind jets and wakes in the lee of Mindoro and Luzon Islands induce the generation and migration of a pair of counter-rotating oceanic eddies in the model, with propagation direction related to the orientation of the winds during each of the surges. Features shared by the eddies include size (100–200 km), depth (~300 m) and propagation speed (0.1–0.15 m s^{-1} for cyclones). Mean wintertime model wind stress positive (negative) curl coincides with the climatological cyclone (anticyclone) distribution from a prior 8-year altimetry-based census of eddies in the southeast quadrant of the South China Sea during the winter monsoon. Moreover, the simulation results agree with contemporaneous satellite and historical *in situ* data characterizing regional oceanic eddy and atmospheric surface jet properties. **Citation:** Pullen, J., J. D. Doyle, P. May, C. Chavanne, P . Flament, and R. A. Arnone (2008), Monsoon surges trigger oceanic eddy formation and propagation in the lee of the Philippine Islands, *Geophys. Res. Lett.*, *35*, L07604, doi:10.1029/2007GL033109.

1. Introduction

[2] Oceanic eddies are common features of island wakes around the world. They have received increased attention from observational programs due to their impact on local biology and chemistry [*Basterretxea et al.*, 2002; *Barton et al.*, 2000]. In Hawaii the interaction of the winds with the topography of the islands creates strong curl patterns that spin-up a field of cyclonic and anticyclonic eddies as a result of Ekman pumping [*Lumpkin*, 1998]. Similar dynamics may be associated with eddies that form in the lee of the Cabo Verde and Canary Islands [*Chavanne et al.*, 2002; *Sangra et al.*, 2007]. The Hawaii, Cabo Verde and Canary Islands are located in the trades where winds have typical values of 6 m s^{-1}, 8 m s^{-1}, and 10 m s^{-1}, respectively, while winds in the jets between the islands can reach 1.5 to 2 times the open ocean values [*Chavanne et al.*, 2002; *Barton et al.*, 2000].

[3] Many island chains are situated in moderate to strong large-scale ocean currents whose fluctuations are implicated in the observed eddy shedding. Instability associated with North Equatorial Current (NEC) flow diverting around the Hawaiian Islands is presumed to induce vortex shedding [*Flament et al.*, 2001], while pulses in the Canary Current (CC) likely generate sequential shedding of oppositely signed vortices behind Gran Canaria [*Sangra et al.*, 2007]. The relative importance of the wind and current in eddy shedding dynamics is, however, not well understood.

[4] To address this gap, modeling studies have illuminated the mechanisms of eddy shedding [*Dong et al.*, 2007]. Process modeling studies suggest that a sufficiently strong incident current (~0.2–0.7 m s^{-1}) can induce eddy separation behind Gran Canaria in the absence of wind; however strong winds (10 m s^{-1}) in the absence of a current are incapable of releasing trapped lee eddies [*Jimenez et al.*, 2008].

[5] Using multi-year altimeter data of the South China Sea (SCS), *Wang et al.* [2003] identified numerous anticyclones positioned to the north of relatively fewer cyclones in the southeast quadrant in winter, but did not hypothesize a forcing mechanism. In our work, realistic high-resolution air-sea modeling is employed to investigate the linkage between the atmospheric dynamics and oceanic eddy genesis and migration in the Philippines region of the SCS. The unique geography of the Philippine Islands effectively isolates the role of topographically-induced wind shear in the ocean response of the island wake region.

2. Model Configuration

2.1. Atmosphere

[6] The atmosphere model COAMPS® [*Chen et al.*, 2003] is configured with 72, 24, and 8 km resolution nests for the western Pacific, with the innermost nest (8 km) covering the Philippines (Figure 1). NOGAPS [*Hogan and Rosmond*, 1991] global atmospheric model fields are used for the initialization (on 1 December 2004) and for boundary conditions on the outermost (72 km) domain at a 6-hour interval. There are 40 terrain-following vertical levels. The model assimilates available quality-controlled observations from aircraft, radiosondes, satellite, ship and surface stations using a multivariate optimum interpolation scheme with a 12 hour incremental update cycle.

2.2. Ocean

[7] The ocean model NCOM [*Martin*, 2000] runs on a domain of 3 km resolution coincident with the COAMPS 8-km nest and uses initial and daily lateral boundary conditions from the ~9 km resolution data-assimilating global HYCOM ocean model [*Chassignet et al.*, 2007]. Eighteen terrain-following coordinates occupy the upper

[1]Naval Research Laboratory, Monterey, California, USA.
[2]Computer Sciences Corporation, Monterey, California, USA.
[3]University of Hawaii at Manoa, Honolulu, Hawaii, USA.
[4]Naval Research Laboratory, Stennis Space Center, Mississippi, USA.

0094-8276/08/2007GL033109

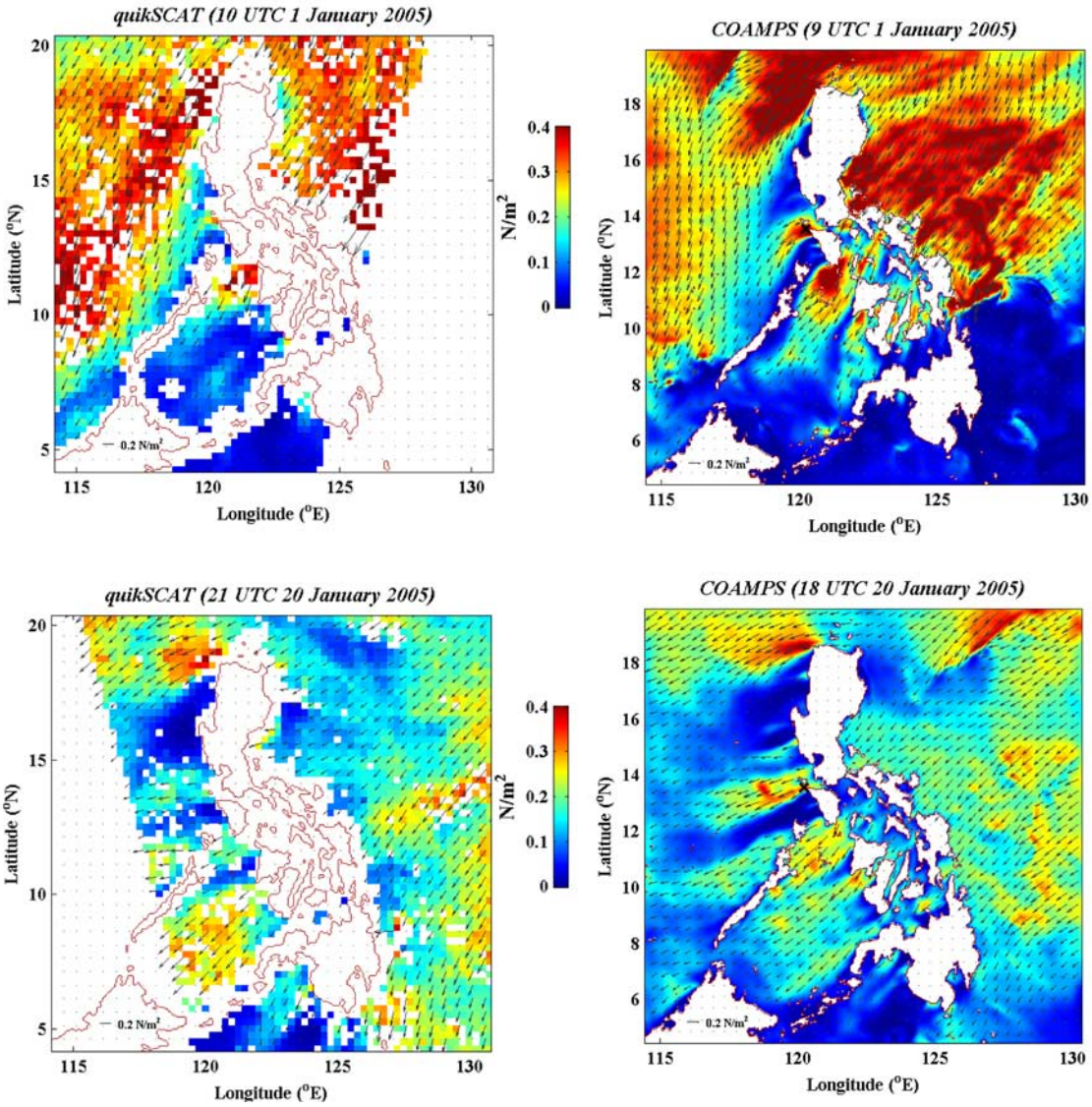

Figure 1. (top) QuikSCAT and COAMPS wind stress during NS. (bottom) Same as above, but for ES. The black cross in the COAMPS panels shows the Mindoro jet location for which statistics are given in the text. QuikSCAT stress arrows are shown every 2nd grid cell; COAMPS stress is interpolated to the NCOM grid and arrows are shown every 15th grid cell.

230 m of the water column, with an additional 18 z-levels extending to the bottom. Hourly momentum and heat fluxes derived from the COAMPS 8 km grid are interpolated bilinearly to the NCOM 3 km grid. The heat fluxes are computed from bulk formulae using the ocean model SST. Additional COAMPS and NCOM model details for a comparable implementation are contained in the work by *Pullen et al.* [2003]. The ocean and atmosphere simulations of the Philippines region encompass three winter months (1 December 2004–28 February 2005).

3. Monsoon Pulsing and Eddy Propagation

3.1. Synoptic Setting

[8] The winter monsoon typically lasts from November to March and is characterized by fairly steady northeasterly winds driven by the Siberian-Mongolian high pressure system. In the Philippines, the monsoon winds interact with the volcanic topography, leading to strong wind jets between islands and through gaps in the rugged terrain. The mean winter (1 December 2004–28 February 2005) 10-m wind speed in the Mindoro wind jet (marked with a cross in Figure 1) is 11 m s^{-1}, with a standard deviation of 3 m s^{-1}.

[9] A strong cold surge swept eastward across the SCS on 1 January 2005, leading to a northerly shift and intensification of monsoon winds. The characteristics of this particular event detailed by *Chang et al.* [2006] fit the definition of a northerly surge (NS) [*Wu and Chan*, 1995, 1997]. QuikSCAT (~25 km resolution) (see *Chavanne et al.* [2002] for data processing details) reveals strong wind stress over the SCS on 1 January 2005, along with intense wind jets in the Philippines (Figure 1). COAMPS wind stress generally agrees with the satellite data in structure and magnitude.

[10] A different kind of monsoon surge occurred on 21 January 2005 with a wind shift to a more easterly orientation. This easterly surge (ES) was initiated by the eastward movement of a high pressure cell over coastal

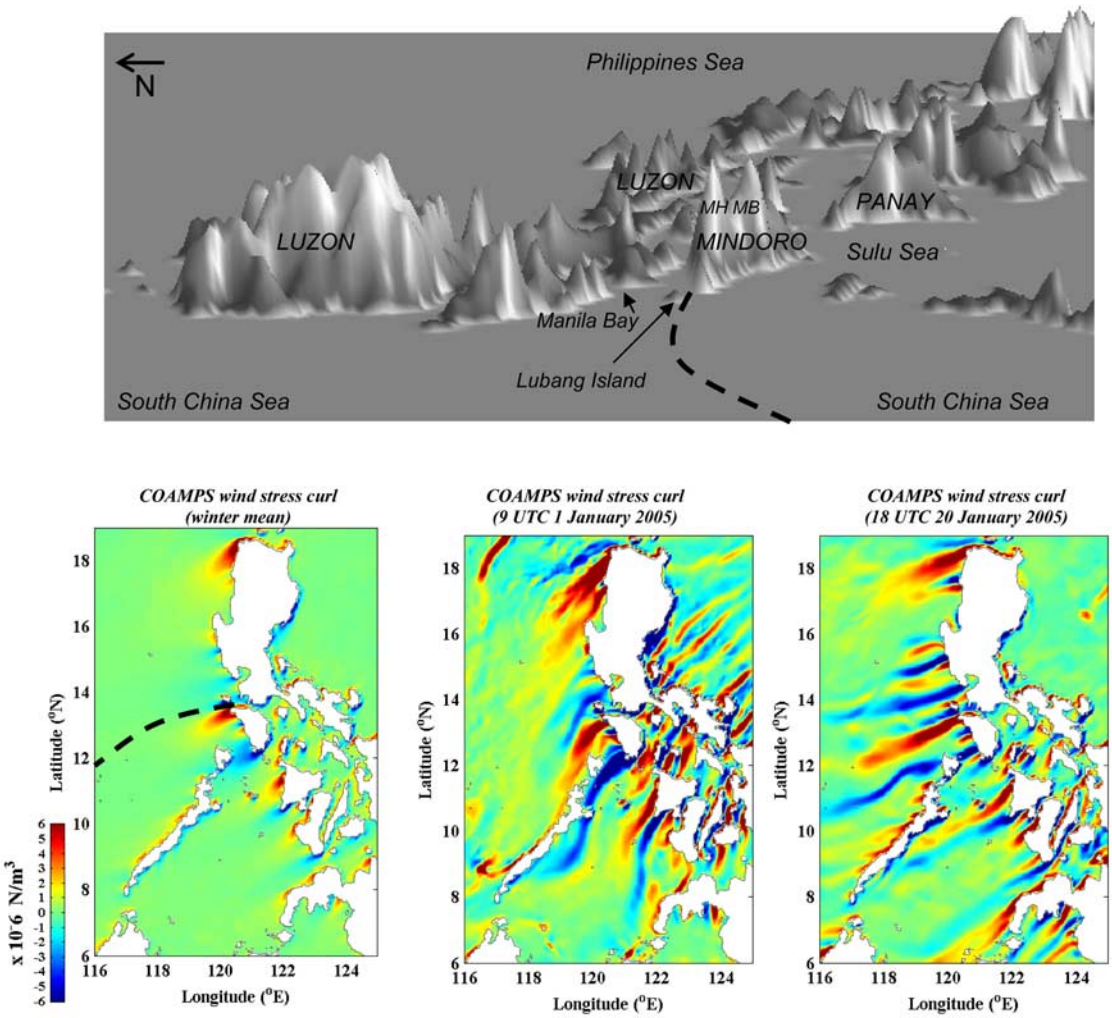

Figure 2. (top) Schematic (viewpoint from the west) showing locations mentioned in the text, including Mindoro's Mount Halcon (MH) and Mount Baco (MB). The black dashed line delineates the zone of cyclones (to the south/right) and anticyclones (to the north/left) found in the work by *Wang et al.* [2003]. US Defense Mapping Agency's 100 m resolution terrain used by 8 km COAMPS is shown. (bottom) COAMPS wind stress curl winter mean (1 Dec 2004–28 Feb 2005), and during NS and ES at the same times as in Figure 1.

China, consistent with previously identified cases of this second type of surge [*Wu and Chan*, 1995, 1997]. The satellite overpass preceded the strongest winds in the model. Nonetheless, the easterly orientation of the monsoon jets is apparent in the QuikSCAT data, and there is reasonable correspondence between the model and observations.

[11] The winds during the surge events are significantly stronger than the seasonal average. Maximum model winds at the Mindoro jet location are 16.6 (15.6) m s^{-1}, while minimum model winds are 11.4 (11.2) m s^{-1} during the NS (ES) event. Mean model winds at the site in the Mindoro jet during the 60 (42) hour NS (ES) event are 14.2 (14.0) m s^{-1}. Winds are relatively steady during the NS (ES) events with standard deviations of 1.6 (1.2) m s^{-1} in the Mindoro jet location.

3.2. Terrain Effects

[12] Mean wintertime positive curl to the right and negative curl to the left (looking downwind) of each island (Luzon, Mindoro, and Panay) is a result of the alternating wind jet and wake pattern and is also observed in the Hawaii, Cabo Verde and Canary island chains [*Chavanne et al.*, 2002; *Barton et al.*, 2000] (Figure 2). The model mean wind stress curl in winter is positive off the northwest tip of Luzon, which is the hypothesized forcing mechanism of the Luzon Cold Eddy [*Qu*, 2000; *Metzger*, 2003] (see auxiliary material[1] Figure S1). A line between the negative curl off southern Luzon and the positive curl off Mindoro (shown on Figure 2) divides anticyclones to the north from cyclones to the south in the altimeter-derived 1993–2000 census of *Wang et al.* [2003]. This axis separating historical anticyclone/cyclone prevalence in winter therefore coincides with the approximate centerline of the Mindoro jet (where the horizontal velocity shear is greatest). The high-resolution (8 km) atmospheric model forcing used in our study facilitates the connection between the terrain-induced

[1]Auxiliary materials are available in the HTML. doi:10.1029/2007GL033109.

wind stress curl field and the historical eddy distribution in the southeast portion of the SCS. Atmospheric model forcing such as NCEP (1°) and ECMWF (1.125°) used in recent SCS ocean modeling studies by *Gan et al.* [2006] and *Metzger* [2003] do not resolve such small-scale curl features.

[13] Whereas the jet and wake lengths were suppressed in the seasonal average due to directional variability of the winds, the wind curl field is intensified and elongated during the two monsoon surge events. Negative (positive) curl values associated with the Mindoro jet reach -15 $(25) \times 10^{-6}$ N m^{-3} during NS and -12 $(15) \times 10^{-6}$ N m^{-3} during ES. The major curl dipoles found off the tips of Mindoro, Luzon and Panay extend downwind approximately 300 km during the NS and ES events, with different orientations during the two events. The positive and negative curl bands are deflected southward on 1 January and westward on 20 January. The wind stress curl upstream of the Philippines on 1 January contains transient striations that are also an intermittent feature of the QuikSCAT data.

[14] Weak winds in island wakes and strong winds in island tip or flank jets [*Doyle and Shapiro*, 1999] are further modified by local topographic effects whose influence is discernible during the two events. The two major peaks on the island of Mindoro, Mt. Halcon and Mt. Baco, both reach a height of ~2500 m and are separated by a shallow pass (Figure 2). In January 2005 the measured inversion height on northern Luzon was approximately 2000–3000 m. The occurrence of an inversion near the mountain-top enhances the lower tropospheric winds in the lee of topography through resonant interactions with the terrain [*Durran*, 1990; *Jiang and Doyle*, 2005]. The small jet accelerated by the Mindoro mountain gap and wakes in the lee of the high terrain, whose surface signature is evident in the wind stress curl field of both events, is a manifestation of such a process.

[15] Elsewhere, details of the curl fields differ between the two events on quite small scales. For example, the negative curl bands offshore of Manila Bay and off the southern tip of Luzon merge in the NS event, whereas during the ES event they remain distinct with Lubang Island generating a small curl couplet in the middle.

3.3. Eddy Propagation

[16] Our model simulation suggests that lee eddies associated with the seasonal monsoon wind forcing are a common feature behind the islands of Luzon and Mindoro. An anticyclone exists in the lee of Luzon before the NS, while a cyclone is present in the lee of Mindoro before the ES (auxiliary material Figure S1). In both cases, the existing eddies are repositioned and strengthened by the monsoon surge and a paired counter-rotating eddy is formed as a result of the surge.

[17] The 1-km resolution MODIS chlorophyll and SST [*Arnone and Parsons*, 2004] reveal a gyre situated immediately to the west of Mindoro more than a week after the NS event of 1 January (Figure 3). The enhanced productivity at the periphery of the cyclone is likely the result of chlorophyll advection from the north side of Mindoro [*Aristegui et al.*, 1997]. An eddy of comparable size (100–200 km), position, and temperature (25–26°C) also appears in the model current and SST fields.

[18] A week after the 21 January ES event, MODIS SST records an ~150 km diameter cold pool to the northwest of Mindoro. The model-derived cyclonic eddy is found in the same location with the same approximate size and temperature. More clearly, a chlorophyll composite image from several weeks after the ES event suggests a double gyre situated about the 14°N latitude line (Figure 3). Enhanced chlorophyll at the cyclone center and on the periphery of the anticyclone are indicative of upwelling (downwelling) and divergence (convergence) of the secondary circulation.

[19] Sea surface temperature gradients associated with the eddies are weak in the model and satellite observations. The dominant temperature signal is the "warm lee" [*Barton et al.*, 2000] in the wake of the islands that is stronger on 27 January relative to 9 January in both satellite and model fields. In the model the diurnal warming in the lee of Mindoro on 27 January is over 1°C, which is weaker than measured by satellite - presumably due to the absence of two-way coupled feedback in the model.

[20] The different eddy positions following the two atmospheric events (west for NS vs. northwest for ES) produced by the model and supported by the satellite data, are suggestive of the influence of the different wind (and wind stress curl) orientations of the two events. Two weeks after the 1 January NS (21 January ES), the resultant paired counter-rotating eddies have migrated southwestward (northwestward) (auxiliary material Figure S1). The cyclonic eddy has become distorted and elongated (possibly as a result of a straining instability) while vorticity more negative than -f makes the anticyclone prone to centrifugal instability until the vorticity reaches -f in the core [*Dong et al.*, 2007]. The cyclone spawned by both events has a propagation speed of ~0.1–0.15 m s^{-1}, which agrees with the rough estimate from successive satellite images. The modeled anticyclone from the NS (ES) moves faster (slower), probably due to interaction with other eddies.

[21] Eddy tracks of the 11 eddies (9 anticyclones and 2 cyclones) observed by satellite altimeter in that quadrant of the SCS in winter months are generally situated to the west and northwest [*Wang et al.*, 2003]. And the eddies in the model are discernible down to at least 300 m, in agreement with hydrographic data taken in an anticyclone in that area in previous years [*Wang et al.*, 2003]. The model thermocline depth is approximately 100 m, with significant shoaling at the site of the cold eddy. The eddies in our model simulations have sea surface height magnitudes of ~5 cm, which is the detection limit for altimetry. These smaller amplitude eddies are thus likely underrepresented by *Wang et al.* [2003].

[22] Vorticity imparted from the overlying wind stress curl appears responsible for the eddy generation and propagation. As a result of the surge, the ocean current accelerates off the northwest tip of Mindoro to the right of the applied wind stress (see Figures 1 and 3). And time-lagged cross-correlations of collocated surface ocean vorticity and wind stress curl for the month of January 2005 are greater than 0.6 in the largest shear zones of the Mindoro jet (see auxiliary material Figure S2).

[23] Whereas the relative contribution of wind and current to eddy shedding is difficult to establish in the case of

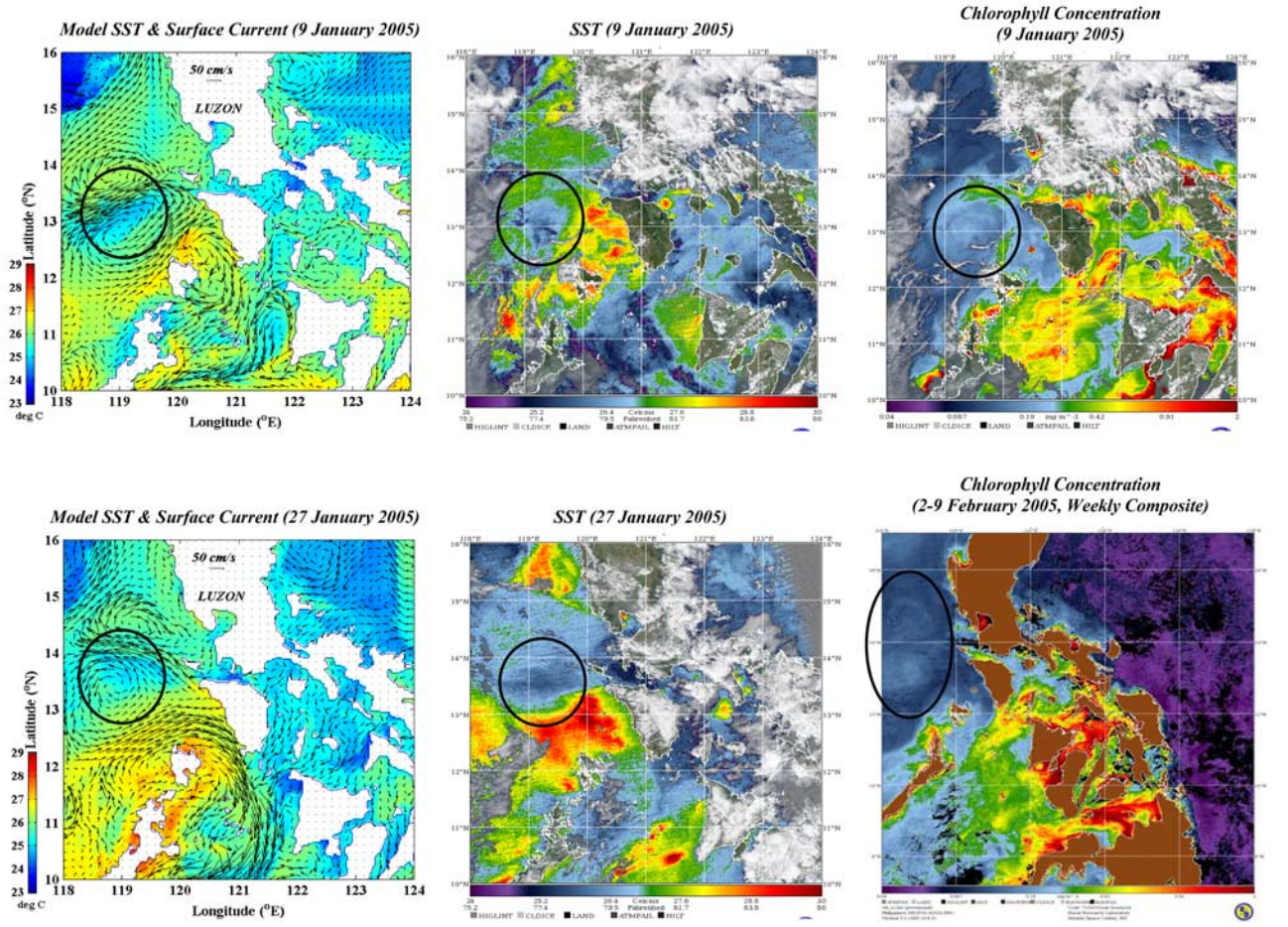

Figure 3. (top) Daytime (14 LT 9 Jan) NCOM SST and surface currents (every 5th grid cell), daytime MODIS SST and chlorophyll. (bottom) Daytime (14 LT 27 Jan) NCOM SST & surface currents (every 5th grid cell), daytime 27 Jan MODIS SST, and composite (2–9 Feb) MODIS chlorophyll.

other island chains, the absence of a background current through the archipelago isolates the role of the wind. For the southeastward extension of Luzon blocks large-scale flow from the Philippines Sea, and the complicated island geometry to the east of Mindoro renders currents in the shallow bays and passages relatively weak and often disorganized, even during strong winds. The differing orientation of the Mindoro wind jet and associated wake regions during each of the surge events influences the direction of the subsequent eddy propagation and highlights the importance of topographically-induced wind shear in forcing the ocean.

4. Discussion

[24] Similar to the ocean/atmosphere interactions of other volcanic island lee regions, the steady monsoon winds interacting with the Philippine islands can form stationary lee eddies. In addition, fluctuations in the monsoon winds induce a dynamic response. Specifically, the local injection of vorticity beneath episodically strengthened wind jets leads to simultaneous detachment of counter-rotating eddies that then migrate in directions dependent on the orientation of the winds: NS (ES) detach eddies that move southwestward (northwestward). The anticyclones survive the longest and are discernible for more than 30 days after the NS and ES events. The properties of the model-produced eddies including temperature (cold eddies of 25°C–26°C), size (100–200 km), depth (300 m), propagation speed (0.1–0.15 m s^{-1} for the cyclones), and the regional distribution of cyclones to the south and anticyclones to the north of a line separating positive/negative wind stress curl extending west from the northern tip of Mindoro, are all consistent with observations in this portion of the SCS.

[25] Monsoon surges are a frequent occurrence during the winter season and have a significant impact on Asian weather. NS and ES each occur one to three times per month during the winter monsoon [*Chang et al.*, 2006; *Wu and Chan*, 1995]. Although not all events propagate a signal as far south as the Philippines, winds in the Mindoro jet during the NS (ES) events examined here achieve speeds 51% (42%) greater than the winter average, with mean winds over the multi-day events exceeding one standard deviation of the winter mean.

[26] Westward-propagating nonlinear mesoscale eddies of 100–200 km diameter and 5–25 cm heights, such as those described here, have recently been established as major contributors to the kinetic energy of the ocean - accounting for over 50% of the mesoscale variability [*Chelton et al.*, 2007]. They serve as conveyors of momentum, heat, and mass as well as biological and chemical

properties. Our investigation suggests that monsoon surges likely represent a robust forcing mechanism for oceanic eddy formation and propagation in the SCS.

[27] **Acknowledgments.** COAMPS® is a registered trademark of the Naval Research Laboratory. Thanks go to Maria Flatau for assistance with the interpretation of monsoon dynamics. Support for J. Pullen, J. Doyle and R. Arnone was provided by Office of Naval Research (ONR) program element 0601153N. C. Chavanne and P. Flament were funded by ONR grant N00014-06-1-0686, NSF grant OCE-0426112, and the State of Hawaii.

References

Aristegui, J., P. Tett, A. Hernandez-Guerra, G. Basterretxea, M. F. Montero, K. Wild, P. Sangra, S. Hernandez-Leon, M. Canton, J. A. Garcia-Braun, M. Pacheco, and E. D. Barton (1997), The influence of island-generated eddies on chlorophyll distribution: A study of mesoscale variation around Gran Canaria, *Deep Sea Res., Part I*, *44*(1), 71–96.

Arnone, R. A., and A. R. Parsons (2004), Real-time use of ocean color remote sensing for coastal monitoring, in *Remote Sensing of the Coastal Environments*, edited by R. L. Miller, C. E. Del Castillo, and B. A. McKee, chap. 14, Kluwer Acad., Norwell, Mass.

Barton, E. D., G. Basterretxea, P. Flament, E. G. Mitchelson-Jacob, B. Jones, J. Aristegui, and F. Herrera (2000), Lee region of Gran Canaria, *J. Geophys. Res.*, *105*(C7), 17,173–17,193.

Basterretxea, G., E. D. Barton, P. Tett, P. Sangra, E. Navarro-Perez, and J. Aristegui (2002), Eddy and deep chlorophyll maximum response to wind-shear in the lee of Gran Canaria, *Deep Sea Res., Part I*, *49*, 1087–1101.

Chang, C.-P., Z. Wang, and H. Hendon (2006), The Asian winter monsoon, in *The Asian Monsoon*, edited by B. Wang, pp. 89–127, Springer, Berlin.

Chassignet, E. P., H. E. Hurlburt, O. M. Smedstad, G. R. Halliwell, P. J. Hogan, A. J. Wallcraft, R. Baraille, and R. Bleck (2007), The HYCOM (HYbrid Coordinate Ocean Model) data assimilative system, *J. Mar. Syst.*, *65*(1–4), 60–83.

Chavanne, C., P. Flament, R. Lumpkin, B. Dousset, and A. Bentamy (2002), Scatterometer observations of wind variations induced by oceanic islands: Implications for wind-driven ocean circulation, *Can. J. Remote Sens.*, *28*(3), 466–474.

Chelton, D. B., M. G. Schlax, R. M. Samelson, and R. A. DeSzoeke (2007), Global observations of large oceanic eddies, *Geophys. Res. Lett.*, *34*, L15606, doi:10.1029/2007GL030812.

Chen, S., et al. (2003), *COAMPS Version 3 Model Description*, 143 pp., Naval Res. Lab., Monterey, Calif.

Dong, C., J. C. McWilliams, and A. F. Shchepetkin (2007), Island wakes in deep water, *J. Phys. Oceanogr.*, *37*, 962–981.

Doyle, J. D., and M. A. Shapiro (1999), Flow response to large-scale topography: The Greenland tip jet, *Tellus, Ser. A*, *51*, 728–748.

Durran, D. R. (1990), Mountain waves and downslope winds, in *Atmospheric Process Over Complex Terrain*, vol. 23, pp. 59–81, Am. Meteorol. Soc., Boston, Mass.

Flament, P., R. Lumpkin, J. Tournadre, and L. Armi (2001), Vortex pairing in an unstable anticyclonic shear flow: Discrete subharmonics of one pendulum day, *J. Fluid Mech.*, *440*, 401–409.

Gan, J., H. Li, E. N. Curchitser, and D. B. Haidvogel (2006), Modeling South China Sea circulation: Response to seasonal forcing regimes, *J. Geophys. Res.*, *111*, C06034, doi:10.1029/2005JC003298.

Hogan, T. F., and T. E. Rosmond (1991), The description of the U. S. Navy Operational Global Atmospheric Prediction System's spectral forecast model, *Mon. Weather Rev.*, *119*, 1786–1815.

Jiang, Q., and J. D. Doyle (2005), Wave breaking induced surface wakes and jets observed during a bora event, *Geophys. Res. Lett.*, *32*, L17807, doi:10.1029/2005GL022398.

Jimenez, B., P. Sangra, and E. Masson (2008), A numerical study of the relative importance of wind and topographic forcing on oceanic eddy shedding by tall deep water islands, *Ocean Modell*, in press.

Lumpkin, C. F. (1998), Eddies and currents of the Hawaiian Islands, Ph.D. thesis, 281 pp., Univ. of Hawaii at Manoa, Honolulu.

Martin, P. J. (2000), A description of the Navy Coastal Ocean Model version 1. 0, *Rep. NRL/FR/7322-00-9962*, 42 pp., Naval Res. Lab., Stennis Space Cent., Miss.

Metzger, J. (2003), Upper ocean sensitivity to wind forcing in the South China Sea, *J. Oceanogr.*, *59*, 783–798.

Pullen, J., J. D. Doyle, R. Hodur, A. Ogston, J. W. Book, H. Perkins, and R. Signell (2003), Coupled ocean-atmosphere nested modeling of the Adriatic Sea during winter and spring 2001, *J. Geophys. Res.*, *108*(C10), 3320, doi:10.1029/2003JC001780.

Qu, T. (2000), Upper-layer circulation in the South China Sea, *J. Phys. Oceanogr.*, *30*, 1450–1460.

Sangra, P., M. Auladell, A. Marrero-Diaz, J. L. Pelegri, E. Fraile-Nuez, A. Rodriguez-Santana, J. M. Martin, E. Mason, and A. Hernandez-Guerra (2007), On the nature of oceanic eddies shed by the Island of Gran Canaria, *Deep Sea Res., Part I*, *54*, 687–709.

Wang, G., J. Su, and P. C. Chu (2003), Mesoscale eddies in the South China Sea observed with altimeter data, *Geophys. Res. Lett.*, *30*(21), 2121, doi:10.1029/2003GL018532.

Wu, M. C., and J. C. L. Chan (1995), Surface features of winter monsoon surges over South China, *Mon. Weather Rev.*, *123*, 662–680.

Wu, M. C., and J. C. L. Chan (1997), Upper-level features associated with winter monsoon surges over South China, *Mon. Weather Rev.*, *125*, 317–340.

J. D. Doyle and J. Pullen, Naval Research Laboratory, 7 Grace Hopper Avenue, Stop #2, Monterey, CA 93943, USA. (julie.pullen@nrlmry.navy. mil)

P. May, Computer Sciences Corporation, 1900 Garden Road, Suite 210, Monterey, CA 93940-5334, USA.

C. Chavanne and P. Flament, University of Hawaii at Manoa, Honolulu, HI 96817, USA.

R. A. Arnone, Naval Research Laboratory, Stennis Space Center, MS 39529-5004, USA.